

NUMERICAL ANALYSIS OF SEMICONDUCTOR THERMOELECTRIC GENERATOR

by

Zhifei WU*, Yuxia XIANG, and Jianjun WANG

School of Mechanical Engineering, Taiyuan University of Technology, Taiyuan, China

Original scientific paper
<https://doi.org/10.2298/TSCI190609025W>

A thermoelectric generation model is proposed based on the structure of thermoelectric generator, working conditions, the effect of air heat transfer and contact resistance in thermoelectric components. In addition, the effect of the thermoelectric generator output performance under the condition of different temperature of the cold and heat source, contact resistance between the cold-end and hot-end, the load resistance and the contact resistance is calculated. The results show that the output voltage is linear associate with the temperature difference between hot and cold ends, however, the output power increase along with the increase of temperature of hot-end and decrease of cold-end. The output voltage reaches 5.76 V and the output power reaches 9.81 W when the temperature difference is 200 °C. Assume that the contact resistance is ignored, the output voltage and power reach peak values of 3.61 V and 3.85 W. The output performance of thermoelectric generator decreases with the increase of thermal contact resistance at hot and cold ends, and the reduction is getting lower and lower. With the increase of the load resistance, the output power increases at the beginning and then decreases. The optimal output power is 3.69 W when the contact resistance is 0 Ω and the optimal load resistance is 3.3 Ω. The maximum output power corresponding to neglecting the contact resistance will be reduced by 13.5% when the contact resistance is 0.5 Ω.

Key words: thermoelectric generation, thermoelectric model, contact resistance, output performance

Introduction

Thermoelectric generator is an independent power source, which is composed of cold source, heat source and thermoelectric module. The low-grade energy and various dissipated heat energy can be converted into electric energy when there is temperature difference between the two ends of thermoelectric module [1]. Ran *et al.* [2] and Deng *et al.* [3] has applied thermoelectric technology to automobiles, using the exhaust heat of automobile exhaust and the waste heat of engines to provide auxiliary power for automobiles, so the utilization rate of fuel is improved. It is also widely used in biomass energy or gas heater to provide electricity for daily life's application [4], and in medical treatment to design a wearable energy capture system to monitor human health [5].

In order to study the output performance of thermoelectric generators, researchers have conducted research on the internal structure parameters and external working conditions of thermoelectric modules. Huland *et al.* [6] concluded that the more logarithm of the coupler arm, the greater output power and the higher energy conversion rate. Liu *et al.* [7] found that the change

* Corresponding author, e-mail: wuzhifei@tyut.edu.cn

of the cross-sectional area of the hot arm had a relatively weak effect on the device conversion efficiency. Erturun *et al.* [8] found that the output power and conversion efficiency of thermoelectric units are greatly affected by the cross-section area and length. Rezaia *et al.* [9] obtained the optimum cross-sectional area ratio of thermocouple pairs by establishing the model. Shi *et al.* [10] finds that changing the geometry or number of thermocouples can only increase the output voltage or current, but cannot increase the output voltage or current at the same time. Experiment shows that the change of temperature and heat transfer conditions at the cold end has little effect on the output performance [11]. At the same time, researchers found that contact pressure, cold source structure and cooling mode also affect the output performance of thermoelectric generator [12-14].

In summary, there are few studies on the influence of temperature and contact effects on the output based on the specific thermoelectric structure. Therefore, this paper proposed the mathematical model of the output performance of thermoelectric generator and the parameters of thermoelectric generator, the temperature of cold and heat source and contact resistance.

Modeling of thermoelectric generation

Model building

When a thermoelectric generator works, the physical properties of thermoelectric module materials will change when the temperature of the cold and hot ends changes. In order to simplify the problem, the following assumptions are made in the process of modeling:

- The Seebeck coefficient, thermal conductivity and resistivity of semiconductor materials are determined by the material properties of P-N junction and the logarithm of thermocouple pairs.
- Ignoring the Thomson effect and the effects of thermal radiation and convection.
- Heat transfer only in 1-D direction, neglecting transverse heat conduction and heat exchange with environment.
- The physical properties of each part of thermoelectric module are fixed and do not change with temperature.
- The thermal conductivity, length, and cross-sectional area of the conductive sheet at the cold and hot end of the thermoelectric module are equal; the thermal conductivity, length, and cross-sectional area of the ceramic substrate at the cold and hot end are equal; and the

thermal conductivity, conductivity, length, and cross-sectional area of the P-type and N-type semiconductor materials are equal.

The thermoelectric generation structure based on the previous assumptions is shown in fig. 1 and the thermoelectric couple model is shown in fig. 2.

The Seebeck coefficient, α , thermal conductivity, K , resistance, R , thermal conductivity of conducting sheet, K_1 , thermal conductivity of ceramic substrate, K_2 and thermal conductivity of air gap, K_3 of thermoelectric module containing m -pair P, N semiconductor thermocouples can be determined by eqs. (1)-(6). Among them, the Seebeck coefficients of semiconductor thermocouples are, respectively, α_p , α_n , the thermal conductivity of semiconductor thermocouples are k_p , k_n , the resistivity are ρ_p , ρ_n , the thermal conductivity of air gap between thermocou-

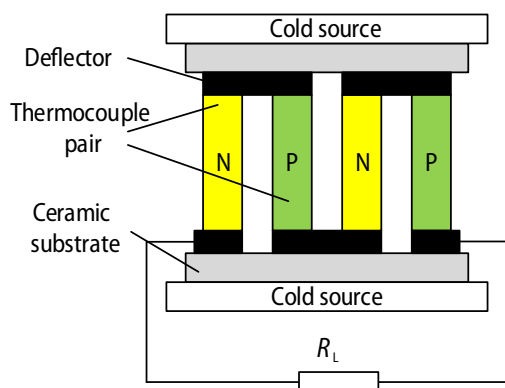


Figure 1. Structure diagram of thermoelectric generator

ple are, respectively, α_p , α_n , the thermal conductivity of semiconductor thermocouples are k_p , k_n , the resistivity are ρ_p , ρ_n , the thermal conductivity of air gap between thermocou-

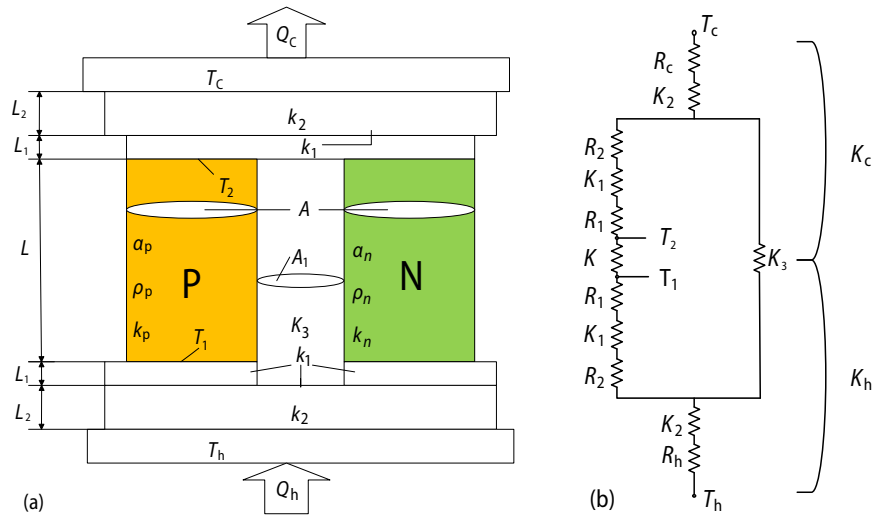


Figure 2. Single-couple model of thermoelectric generation; (a) structure schematic diagram of couples; (b) thermal conductivity and thermal resistance schematic diagram of thermoelectric generators

ples is k_3 , the length of the arm of the couple is L , the thickness of the conducting plate at the cold or hot end is L_1 , the thickness of the ceramic substrate at the cold or hot end is L_2 , the cross-sectional area of P or N type couples is A , the cross-sectional area of the air gap between the single couple is A_1 , cross-sectional area of ceramic substrates at cold or hot ends is A_2 :

$$\alpha = m(\alpha_p - \alpha_n) \quad (1)$$

$$K = \frac{mA(k_p + k_n)}{L} \quad (2)$$

$$R = \frac{mL(\rho_p + \rho_n)}{A} \quad (3)$$

$$K_1 = \frac{m(2A + A_1)k_1}{L_1} \quad (4)$$

$$K_2 = \frac{k_2 A_2}{L_2} \quad (5)$$

$$K_3 = \frac{(A_2 - 2mA)k_3}{L} \quad (6)$$

According to the principle of resistance superposition, the thermal conductivity formula of the cold and hot end of thermoelectric generator can be obtained:

$$K_h = K + K_1 + K_2 + K_3 + \frac{1}{R_1} + \frac{1}{R_2} + \frac{1}{R_h} \quad (7)$$

$$K_c = K + K_1 + K_2 + K_3 + \frac{1}{R_1} + \frac{1}{R_2} + \frac{1}{R_c} \quad (8)$$

where K is the thermal conductivity of thermocouple pairs of thermoelectric generators, K_1 – the thermal conductivity of copper sheets at the cold or hot ends of thermoelectric modules, K_2 – the thermal conductivity of ceramic substrates at the cold or hot ends, K_3 – the total thermal conductivity of air gap of thermoelectric modules, R_1 – the contact resistance between semiconductor materials between the cold or hot ends and conductive sheets, R_2 – the contact thermal resistance between the cold or hot end conductive sheets and ceramic substrates, R_h, R_c respectively represent the contact thermal resistance between the ceramic substrate and the heat source and the cold source.

According to the heat transfer principle, the energy conversion principle of thermoelectric module can be expressed by eqs. (9)-(11), which Q_h is the heat absorbed by the hot end of thermoelectric module from the heat source, Q_c – the heat flowing into the cold end of thermoelectric module to the cold source, Q_{tm} – the heat transmitted through the thermocouple pair and air gap:

$$Q_h = K_h (T_h - T_1) \quad (9)$$

$$Q_c = K_c (T_2 - T_c) \quad (10)$$

$$Q_{tm} = (K + K_3) \cdot (T_1 - T_2) \quad (11)$$

When there is a temperature difference between the two ends of the thermoelectric module, the thermoelectric module is equivalent to a power supply. The Joule heat will be generated in the circuit due to the current passing through, according to the heat balance, the energy balance equations of the hot end and the cold end of the thermoelectric generator can be expressed:

$$Q_h = m\alpha T_1 I + Q_{tm} - \frac{1}{2} I^2 (R + R_t) \quad (12)$$

$$Q_c = m\alpha T_2 I + Q_{tm} - \frac{1}{2} I^2 (R + R_t) \quad (13)$$

Among them, R_t is the contact resistance, which consists of the resistance of the guide plate of the thermoelectric module and the contact resistance of the guide plate and the thermocouple.

According to the Seebeck effect, the total voltage generated by the thermoelectric generator and the current in the circuit can be derived:

$$U = \alpha (T_1 - T_2) \quad (14)$$

$$I = \frac{U}{R_L + R_t + R} \quad (15)$$

where R_L is the load resistance of the series thermoelectric generator.

According to the principle of conservation of energy, the output voltage U_1 and output power P of thermoelectric generator system can be expressed:

$$U_1 = IR_L \quad (16)$$

$$P = (Q_h - Q_c) = U_1 I \quad (17)$$

Simultaneous eqs. (1)-(17) can available:

$$I = \frac{m(\alpha_p - \alpha_n)(T_h - T_c)}{m^2(\alpha_p - \alpha_n)^2 \left(\frac{T_h}{B + \frac{L}{R_c}} + \frac{T_c}{B + \frac{L}{R_h}} \right) + \left[1 + \frac{mA(k_p + k_n)}{B + \frac{L}{R_h}} + \frac{mA(k_p + k_n)}{B + \frac{L}{R_c}} \right] \left[R_L + \frac{mL(\rho_p + \rho_n)}{A} + R_t \right]} \quad (18)$$

$$U_1 = \frac{m(\alpha_p - \alpha_n)(T_h - T_c)R_L}{m^2(\alpha_p - \alpha_n)^2 \left(\frac{T_h}{B + \frac{L}{R_c}} + \frac{T_c}{B + \frac{L}{R_h}} \right) + \left[1 + \frac{mA(k_p + k_n)}{B + \frac{L}{R_h}} + \frac{mA(k_p + k_n)}{B + \frac{L}{R_c}} \right] \left[R_L + \frac{mL(\rho_p + \rho_n)}{A} + R_t \right]} \quad (19)$$

Model verification

In order to verify the accuracy of the model, [15] medium temperature differential generator parameters and experimental conditions, the model is used to simulate the power generation performance. The material performance and structure parameters for simulation are shown in tab. 1. Assumed that the contact resistance between the thermoelectric module and the cold and hot end is zero, the internal contact resistance is 0.1 Ω , the load resistance is 3.4 Ω , and the temperature of the cold and hot end is 25 $^{\circ}\text{C}$ and 145 $^{\circ}\text{C}$, respectively. The simulation results are shown in tab. 2.

Table 1. Material properties and structural dimensions used for model validation

Characteristic	Thermocouple material	Deflector	Ceramic substrate	Air gap
Seebeck coefficient [VK^{-1}]	$226.8 \cdot 10^{-6}$	$6.5 \cdot 10^{-6}$	—	—
Conductivity [Ωm^{-1}]	$1.447 \cdot 10^{-5}$	$5.81 \cdot 10^7$	—	—
Thermal conductivity [$\text{Wm}^{-1}\text{K}^{-1}$]	1.52	386	130	0.03
Thickness [m]	$1.6 \cdot 10^{-3}$	$2 \cdot 10^{-4}$	$6 \cdot 10^{-4}$	$1.8 \cdot 10^{-3}$
Acreage [m^2]	$1.96 \cdot 10^{-6}$	$8 \cdot 10^{-7}$	$1.6 \cdot 10^{-1}$	$2.5 \cdot 10^{-7}$

It can be seen from tab. 2, compared with the experimental data in the literature, the simulation results show that the output current error is 5% and the output power error is 7.7%, with a deviation of less than 10%, indicating that the model has a high accuracy and can be used for subsequent trial analysis.

Table 2. Comparison of numerical analysis results

Contrastive terms	Simulation result	Experiment data
Output current	1.026	1.08
Output power	3.58	3.88

Result and discuss

Hot and cold end temperature

The thermal contact resistance of the hot and cold end was neglected in the numerical simulation process. Figures 3 and 4 are the relationship between output voltage, output power and the temperature of the hot and cold end.

It can be seen from fig. 3 that the output voltage has a linear relationship with temperature. This is because the temperature of the cold source remains unchanged, the temperature difference between the cold end and the hot end increases. As a result, the electron mobility of

thermocouples increases, the positive and negative electrons accumulated at both ends of PN semiconductor increase, which ultimately leads to a larger output voltage. When the temperature difference is fixed, the temperature difference at the cold and hot ends will also affect the output voltage.

Figure 4 shows that when the temperature of cold source is fixed, the output power increases with the increase of the temperature of heat source. This is because the increase of the temperature of heat source leads to the increase of the heat absorbed by thermocouples, which increases the output power of the thermoelectric generator. The temperature of cold end is 0 °C, and the hot end temperature 200 °C is 7.3 W higher than that of the hot end temperature is 100 °C.

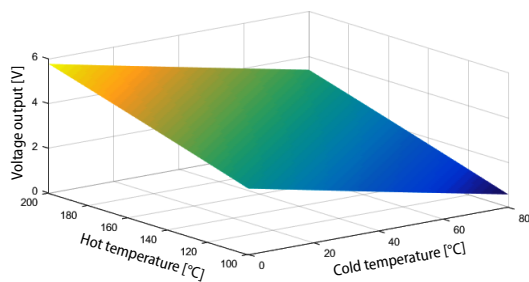


Figure 3. The effect of temperature change at hot and cold ends on the output voltage

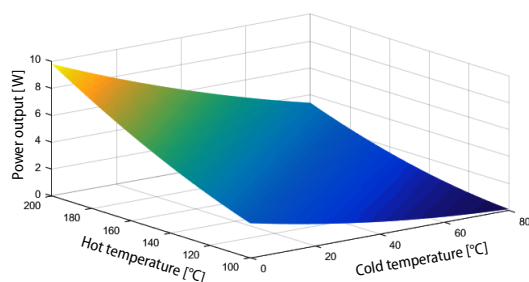


Figure 4. The effect of temperature change at hot and cold ends on output power

Contact resistance at hot and cold ends

The temperature of cold and hot end of thermoelectric generator is set to 25° and 145°, respectively, the load resistance is 3.4 Ω, the internal contact resistance is 0.1 Ω, and the change range of contact resistance at cold and hot end is 0-0.2 Ω. Figures 5 and 6 are, respectively, the change curves of output voltage and output power with the contact resistance of the cold and hot ends.

According to fig. 6, if there is no contact resistance at the cold and hot ends, the output power reaches a peak value of 3.58 W, and then the output voltage begins to decrease with the increase of the contact resistance at the cold and hot ends. When the contact resistance at the cold and hot ends are both 0.2 Ω, the power output value decreases by 14% compared with 3.58 W.

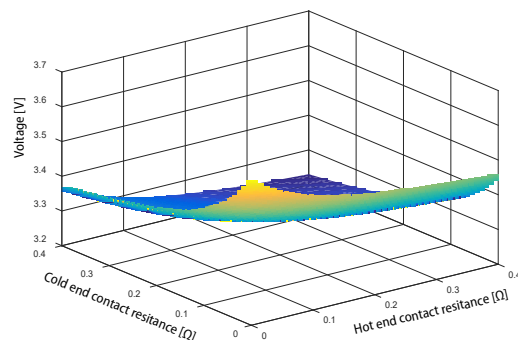


Figure 5. The effect of the change of contact resistance at hot and cold ends on the output voltage

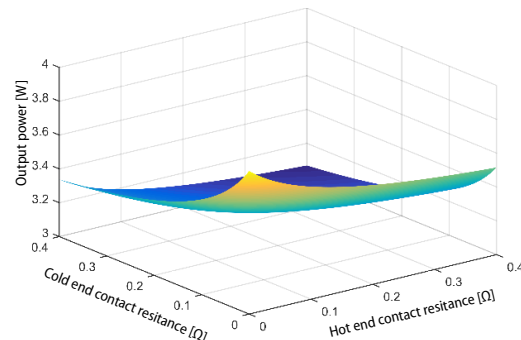


Figure 6. The effect of the change of contact resistance at hot and cold ends on the output power

Conclusion

Based on the structure and working conditions of thermoelectric generation, this paper establishes a thermoelectric generation model of semiconductor, and obtains the relationship between the output voltage of thermoelectric generator and the output power and other factors. Through numerical simulation, the output characteristics of thermoelectric generator are analyzed, and the linear relationship between the output voltage and the temperature of cold and heat sources is obtained, and the contact resistance of the cold and hot ends will affect the output performance of the thermoelectric generator. With the increase of the contact resistance of the cold and hot ends, the output performance will decrease first and then remain unchanged, so the smooth contact surface should be ensured as far as possible through analysis.

Acknowledgment

The authors are grateful for the supported by the Shanxi Province Science and Technology Major Project (Grant No. 20181102006).

References

- [1] He, W., et al., Recent Development and Application of Thermoelectric Generator and Cooler, *Applied Energy*, 143 (2015), Apr., pp. 1-25
- [2] Ran, Y., et al., Energy Efficient Thermoelectric Generator-Powered Localized Air-Conditioning System Applied in a Heavy-Duty Vehicle, *Journal of Energy Resources Technology*, 140 (2018), 7, 072007
- [3] Deng, Y. D., et al., Fuel Economy Improvement by Utilizing Thermoelectric Generator in Heavy-duty Vehicle, *Journal of Electronic Materials*, 46 (2017), 5, pp. 3227-3234
- [4] O'Shaughnessy, S. M., et al., Adaptive Design of a Prototype Electricity-Producing Biomass Cooking Stove, *Energy for Sustainable Development*, 28 (2015), Oct., pp. 41-51
- [5] Kim, C. S., et al., Structural Design of a Flexible Thermoelectric Power Generator for Wearable Applications, *Applied Energy*, 214 (2018), Mar., pp. 131-138
- [6] Hyland, M., et al., Wearable Thermoelectric Generators for Human Body Heat Harvesting, *Applied Energy*, 182 (2016), Nov., pp. 518-524
- [7] Liu, L., et al., Modeling of Flat-Plate Solar Thermoelectric Generators for Space Applications, *Solar Energy*, 132 (2016), July, pp. 386-394
- [8] Erturun, U., et al., Influence of Leg Sizing and Spacing on Power Generation and Thermal Stresses of Thermoelectric Devices, *Applied Energy*, 159 (2015), Dec., pp. 19-27
- [9] Rezaia, A., et al., Parametric Optimization of Thermoelectric Elements Footprint for Maximum Power Generation, *Journal of Power Sources*, 255 (2014), 255, pp. 151-156
- [10] Shi, Y., et al., A Real-Sized Three-Dimensional Numerical Model of Thermoelectric Generators at a Given Thermal Input and Matched Load Resistance, *Energy Conversion & Management*, 101 (2015), Sept., pp. 713-720
- [11] Navarro-Peris, E., et al., Evaluation of the Potential Recovery of Compressor Heat Losses to Enhance the Efficiency of Refrigeration Systems by Means of Thermoelectric Generation, *Applied Thermal Engineering*, 89 (2015), Oct., pp. 755-762
- [12] Wang, S., et al., Experimental Study of the Effects of the Thermal Contact Resistance on the Performance of Thermoelectric Generator, *Applied Thermal Engineering*, 130 (2018), Feb., pp. 847-853
- [13] Akyildiz, F. T., Vajravelu, K., Galerkin-Chebyshev Pseudo Spectral Method and a Split Step New Approach for a Class of Two Dimensional Semi-Linear Parabolic Equations of Second Order, *Applied Mathematics & Nonlinear Sciences*, 3 (2018), 1, pp. 255-264
- [14] Zhu, L., et al., Affine Transformation Based Ontology Sparse Vector Learning Algorithm, *Applied Mathematics & Nonlinear Sciences*, 2 (2017), 1, pp. 111-122
- [15] Liao, M., et al., A Three-Dimensional Model for Thermoelectric Generator and the Influence of Peltier Effect on the Performance and Heat Transfer, *Applied Thermal Engineering*, 133 (2018), pp. 493-500